

Article

Simulation Study on the Combustion and Emissions of a Diesel Engine with Different Oxygenated Blended Fuels

Xiuzhen Li ¹, Qiang Liu ^{2,*}, Yanying Ma ¹, Guanghua Wu ², Zhou Yang ² and Qiang Fu ²

¹ School of Data Science and Artificial Intelligence, Jilin Engineering Normal University, Changchun 130052, China; lxx540860393@126.com (X.L.); mayanying@jlnu.edu.cn (Y.M.)

² School of Mechanical and Vehicular Engineering, Jilin Engineering Normal University, Changchun 130052, China; wgh5668@126.com (G.W.); nanfengzhou@yeah.net (Z.Y.); fuqiang718@126.com (Q.F.)

* Correspondence: liuqiang@jlnu.edu.cn

Abstract: Aiming to achieve the goal of efficient and clean combustion in internal combustion engines, simulations are used to change the physicochemical properties and molecular configuration of fuels by adding oxygenated fuels such as alcohols, esters, ethers, etc., so as to achieve the purpose of improving combustion and reducing emissions. In this paper, blends of oxygenated fuels, including n-butanol, DME, DMC, and diesel fuel with different oxygen-containing functional groups, were selected for simulation to reveal the chemical mechanisms of fuel oxygen on combustion and pollutant generation in the combustion system and to deeply explore the mechanism and influence law of the different forms of oxygen bonding on the generation and oxidation of carbon smoke. At the same fuel oxygen content, the differences in the fuel physicochemical properties and reaction paths resulted in different effects of the different oxygenated fuels on the in-cylinder oxidative activity and different inhibition abilities of carbon smoke precursors. Compared with pure diesel, n-butanol, and DME, which promoted OH generation, DMC inhibited OH generation, so the oxidation activity of diesel/n-butanol was the highest, and that of diesel/DMC was the lowest; meanwhile, the two O atoms in the DMC molecule formed CO₂ with one C atom, which reduced the utilization efficiency of the O atoms, whereas each O atom in the n-butanol and DME fuels took away one C atom, so the utilization efficiency of O atoms was higher. The individual oxygenated fuels themselves had different abilities to contribute to carbon smoke precursors, and the above combined factors led to reductions of 8.7%, 32.6%, and 85.4% in soot emissions from the addition of DMC, DME, and n-butanol compared to pure diesel fuel, respectively, at the same oxygen content. At a medium load, the addition of n-butanol, DME, and DMC reduced NO_x emissions by 0.5%, 1.7%, and 3.3%, respectively. Thus, it is shown that DMC has a more significant effect on NO_x emission reduction.

Keywords: diesel engine; oxygenated fuel; soot; NO_x; CO



Citation: Li, X.; Liu, Q.; Ma, Y.; Wu, G.; Yang, Z.; Fu, Q. Simulation Study on the Combustion and Emissions of a Diesel Engine with Different Oxygenated Blended Fuels. *Sustainability* **2024**, *16*, 631. <https://doi.org/10.3390/su16020631>

Academic Editors: Francesco Nocera and Adam Smoliński

Received: 6 September 2023

Revised: 23 December 2023

Accepted: 4 January 2024

Published: 11 January 2024



Copyright: © 2024 by the authors. Licensee MDPI, Basel, Switzerland. This article is an open access article distributed under the terms and conditions of the Creative Commons Attribution (CC BY) license (<https://creativecommons.org/licenses/by/4.0/>).

1. Introduction

In the past 100 years since its invention, the internal combustion engine has undergone continuous improvement and development and is widely used in many fields, such as in automobiles and agricultural machinery, due to its wide range of adaptability, high reliability, and high thermal efficiency. However, the massive use of internal combustion engines has also brought about negative problems that cannot be ignored, with the energy crisis and environmental pollution being the main challenges. In recent years, due to the increasingly stringent emission regulations and people's increasing awareness of environmental protection, many scholars at home and abroad have devoted themselves to exploring ways to reduce pollutant emissions from diesel engines [1]. Presently, the commonly utilized clean alternative fuels primarily encompass gas fuels, synthetic oils, and oxygenated fuels. Among these, the oxygenated fuels frequently employed in diesel engines primarily consist of alcohols, esters, and ethers.

Methanol and ethanol are mostly used in gasoline engines due to their high octane numbers, and engines burning ethanol gasoline can withstand higher compression ratios, which is conducive to improving their economy and dynamics. Vargün M. [2] investigated the effect of fuel injection stages on the combustion and exhaust characteristics of a diesel engine using an alcohol–diesel mixture. The results of the study showed that the cylinder gas pressure was improved by advancing the injection time. Also, the heat release rate increased as the alcohol content in the fuel blend increased. In addition, the combustion duration of the alcohol–diesel blends was significantly shorter. The use of fuel blends resulted in a significant reduction in CO and NH₃ emissions. In addition, changing the fuel injection time was found to be effective in reducing CO₂ and NO_x emissions. Yilbaşı Z, Yeşilyurt M K, and Arslan M et al. [3] investigated the effects of biodiesel vegetable oil, alcohol, and diesel fuel on the diesel combustion and emissions of tetrad blends. The engine test results showed that the brake-specific fuel consumption of the blends increased by 4.54% to 27.82% compared to diesel fuel, but the brake thermal efficiency decreased due to its lower calorific value. The overall emission values of all the tested blends were reduced compared to diesel fuel. The combustion characteristics showed that the addition of various alcohols to ternary blends resulted in higher in-cylinder pressures and lower heat release rates. It was concluded that diesel–biodiesel–vegetable and oil–pentanol blends are suitable for improved performance, combustion properties, and reduced exhaust emissions. Yesilyurt M. K. [4] studied the effect of diesel–safflower-oil biodiesel binary blends and diesel–biodiesel–pentanol ternary blends on the performance, emission, and combustion characteristics of diesel generators. The results showed that the ternary blends significantly reduced the brake thermal efficiency (BTE) and simultaneously increased the brake specific fuel consumption (BSFC) by up to 13.90% compared to diesel. In addition, the increase in the pentanol concentration had a significant effect on the reduction in NO_x emissions. It is worth noting that the addition of pentanol to diesel–biodiesel blends reduces emissions, while CO emissions increase significantly due to the excess oxygen content that allows for more complete combustion.

Commonly used ether fuels mainly include dimethyl ether (DME) with the molecular formula CH₃OCH₃. DME does not contain C–C bonds in its molecular structure, which can better inhibit the generation of carbon soot precursors, and with a mass fraction of oxygen of 34.8%, it can promote the oxidation of carbon soot in the later stages of combustion. Ping Sun [5] studied the particle number (PN) and particle size distribution of a combined DME/gasoline injection spark-ignition engine, which was experimentally investigated, and the percentages of DME were 0, 5%, 10%, 15%, and 20%. The results show that the addition of DME can effectively reduce the particle number of DME/gasoline engines in both the accumulation and nucleation modes compared to pure gasoline engines. Most of the particles in the DME/gasoline engine were sized in the nucleation mode, with a peak value of about 17.8 nm at different ignition timings and DME ratios. Both the nucleated particle number (NPN) and accumulated particle number (APN) were related to the operating conditions investigated in this study, and the extent of their effects depended on the DME ratio. The APN fraction was almost the same for pure gasoline but increased with the addition of dimethyl ether as the engine load increased. Putrasari Y [6] believes that DME is a new-generation fuel derived from natural gas and coal. This fuel can be used directly in conventional internal combustion (IC) engines without any major modifications. The main advantage of DME combustion in IC engines is its low NO_x and particulate emissions compared to fossil liquid fuels. Therefore, the use of DME in IC engines has the potential to improve engine efficiency and reduce emissions in the future without much experimentation. This paper provides a comprehensive review of some of the topics related to the use of DME as an alternative fuel for IC engines and efforts to increase the utilization of DME to meet future high-efficiency and low-emission regulations. Yilbaşı Z et al. [7] studied the effect of biodiesel–diesel–advanced-alcohols (1-pentanol, 1-hexanol, and 1-heptanol) blends on the performance, emission, and combustion behavior of a single-cylinder diesel engine. For the tests, 80% diesel and 20% hemp

seed oil biodiesel were blended and named B20. The biodiesel fuel was produced by transesterification from hemp seed oil in the presence of methanol and potassium hydroxide for the preparation of the B20 binary test fuel and other ternary fuels. In addition, nine ternary blends (20% HSOB plus 70%, 60%, and 50% diesel, respectively, plus 10%, 20% and 30% higher alcohol (pentanol, hexanol, and heptanol), respectively) were prepared. By comparing the experimental data of the different ternary blends, it was concluded that the increase in the alcohol concentration in the blends delayed the onset of combustion, and therefore the ignition delay was prolonged. In terms of the fuel line pressure data, the observed changes depended on the quantity, viscosity, and density of the fuel. The addition of biodiesel and high alcohols to the diesel fuel resulted in lower NO_x, CO, unburned hydrocarbons, and smoke emissions and increased CO₂ emissions. The values of NO_x, CO, and unburned HC at full load were lower for the higher-alcohol blends as compared to diesel fuel and were 3.04–22.24%, 22.85–56.35%, and 5.44–22.83%, respectively.

The main characteristic of ester fuels is that they contain carbon–oxygen double bonds. The ester fuels that are more frequently used in diesel engines are mainly biodiesel and dimethyl carbonate (DMC) [8]. Compared with fossil diesel, biodiesel does not contain aromatic hydrocarbon components and contains oxygen, which can inhibit the generation of carbon soot in the combustion process and is a clean fuel. N. Usta et al. [9] synthesized a methyl ester biodiesel with a higher viscosity than diesel oil using hazelnut oil and sunflower oil as the raw materials and blended this biodiesel in a supercharged diesel engine for experimental studies. The studies showed an increase in torque and power at full and partial loads, despite the lower calorific value of the blended fuel compared to fossil diesel. The maximum power and thermal efficiency were achieved when the biodiesel blending percentage was 17.5%.

Moreover, due to varying prime compression ratios among fuels, a specific fuel must be chosen for optimization in a dual-fuel engine. Variable compression ratios (VCRs) enable the engine's compression ratio to be optimized for each fuel. The globally produced Dongfeng Nissan's new VC-Turbo 2.0-liter turbocharged motor unveiled at the 2017 Los Angeles Auto Show represents a significant advancement in traditional engine technology. Providing a 12% increase in fuel economy, a peak power of 185 kW, and a peak torque of 380 N·m and being complemented by an electric torque rod for balancing vibration from the variable compression ratio system, the new VCR engine demonstrates notable advances.

Conventional diesel engines have limited potential to achieve ultra-low emissions due to short their oil–gas mixing time and uneven mixture, so exploring efficient and clean combustion technology is one of the important tasks for internal combustion engine workers. Therefore, this study is aimed at the goal of the efficient and clean combustion of internal combustion engines, using a combination of experiments and simulations to change the physicochemical properties and molecular configuration of fuels by adding alcohols, esters, ethers, and other oxygenated fuels to improve the combustion and reduce emissions and to investigate the influence of oxygen elements in fuels and the structure of different oxygenated functional groups on the combustion and pollutant generation and chemical mechanisms.

2. Test System and Test Conditions

A schematic diagram of the engine stand is illustrated in Figure 1. The test was carried out on a 4-cylinder supercharged, intercooled, electronically controlled, high-pressure, common-rail, high-speed diesel engine with a displacement of 2.771 L. Table 1 shows the main technical parameters of the machine [10]. The main measurement and control systems of the engine test bench included an eddy current dynamometer, combustion analyzer, air flow meter, and so on. The INCA V7.2.17 software and the open ECU allowed the flexible adjustment of fuel injection parameters such as the fuel injection quantity, fuel injection timing, and rail pressure of the high-pressure standard rail fuel injection system controlled by the Bosch electronic control unit. The cylinder pressure was measured by a Kistler

6052 C cylinder pressure transducer with a sampling interval of 0.1 °CA. To eliminate measurement errors, an average of 100 cycles of cylinder pressure was collected at each operating point. To ensure the repeatability and comparability of the test data, the test was repeated five times during the test, the highest and lowest values were removed, and the average of the remaining values was calculated. In addition, the cooling water temperature was controlled at 85 ± 3 °C, the intake air temperature was kept at (30 ± 2) °C, the engine speed was 1800 r/min, and the engine load was 50% of the full load. In the test, it was ensured that the amount of circulating oil supply under the same load was the same. Throughout the test, it was confirmed that the amount of circulating oil supply under identical load was the same.

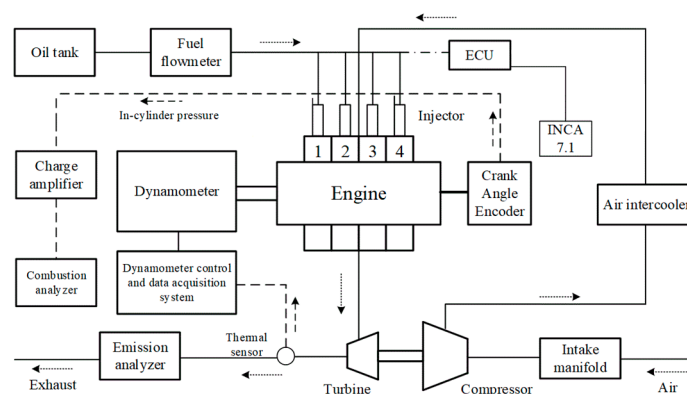


Figure 1. Schematic diagram of the engine stand.

Table 1. Main technical parameters of the engine.

Parameter	Value
Stroke	102 mm
Bore	93 mm
Compression ratio (CR)	17.2
Engine Type	Turbocharged Four-cylinder
Cooling method	Water cooling
Rated speed	3400
Number of holes	4
Rated power	82 kW

First, the injection pressure was fixed at 140 MPa, and the main injection timing was fixed at -8.5 °CA ATDC to study the effect of the diesel fuel on the combustion of the diesel engine, and the cylinder pressure data were recorded. Subsequently, the operating conditions were kept constant, and the diesel fuel was replaced to study the effect of n-butanol-blended diesel fuel, i.e., n-butanol/diesel fuel (oxygen content at an n-butanol blend ratio of 30%), on the combustion, and the cylinder pressure data were recorded. Then, the operating conditions were kept constant, and the n-butanol/diesel fuel was replaced to study the effect of dimethyl ether (DME)-blended diesel fuel, i.e., DME/diesel fuel (oxygen content at a DME blend ratio of 18.6%), on the combustion, and the cylinder pressure data were recorded. Then, the working conditions were kept unchanged, and the DME/diesel fuel was replaced to study the effect of DMC-blended diesel fuel, i.e., DMC/diesel fuel (oxygen content at DMC blend ratio of 12.2%), on the combustion, and the cylinder pressure data were recorded.

In this study, the blends of oxygenated fuels, i.e., n-butanol, DME, and DMC, with diesel fuel with different oxygenated functional groups were selected for the combination of experiments and simulations, and it was ensured that all three blends had an elemental mass fraction of oxygen of 6.49% and that the blending ratios of the oxygenated fuels in the

three blends were different, but the overall elemental mass fraction of the fuels in terms of C was close to each other, and their calorific values were not much different.

The diesel engine combustion chamber was symmetrical, and in order to improve the calculation efficiency, the calculation area was set to 1/6 of the whole combustion chamber according to the number of spray holes (the top view is a 60° sector). The model is shown in Figure 2.

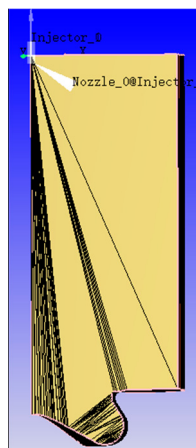


Figure 2. Three-dimensional mesh of the combustion chamber.

The turbulence model of this paper selected the RNG $k-\epsilon$ model under the Reynolds time-averaged N-S equation. The study of this paper focused on the detailed process of emission pollutant generation, and the 3D simulation model needed to couple the chemical reaction mechanism to achieve the required computational accuracy, so the SAGE chemical reaction solver model was selected. In the PM (particulate mimic) model in the detailed carbon soot model, PAH (polycyclic aromatic hydrocarbon) was selected as the carbon soot precursor [11]. The extended Zeldovich model was used in this study regarding NO_x modeling. The CONVERGE_Studio_v3.0 software was used based on the discrete droplet model (DDM) to describe the spraying process in the cylinder, and the individual computational models selected in this paper are shown in Table 2.

Table 2. Spray models used for calculations.

Parameter	Model	Parameter	Model
Spray fragmentation	KH-RT	Droplet wall	Rebound/slide
Turbulent diffusion	O'Rourke	Droplet evaporation	Frossling
Droplet collision	NTC	Collision result processing	Post composite model

In this study, the blends of the oxygenated fuels, i.e., n-butanol, DME, DMC, and diesel with different oxygen-containing functional groups were selected for simulation, and the oxygen mass fraction of all three blends was ensured to be 6.49% (oxygen content at 30% n-butanol blending ratio), and the calculation working conditions were still 1800 r/min at a 50% load, and the simulation calculation shown in Table 3 shows the series of physical parameters of diesel (n-heptane), n-butanol, DME, and DMC to ensure the same amount of circulating fuel supply under the same load. Table 4 shows the physicochemical properties of the three fuel blends under the same fuel oxygen content. Table 5 summarizes the resolution and uncertainty of the main instruments used in this study.

Table 3. Comparison of physicochemical properties of different oxygenated fuels.

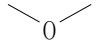
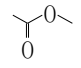
Properties	Diesel Fuel (n-Heptane)	n-Butanol [12]	DME [13]	DMC [14]
Molecular formula	C ₇ H ₁₆	C ₄ H ₉ OH	CH ₃ OCH ₃	CH ₃ OCOCH ₃
Oxygen-containing functional group structure	None	—OH		
CN	40–55	12	55–60	35–36
Calorific value/MJ.kg ^{−1}	42.5 (44)	35.1 (36)	28.4	15.78
Oxygen content %	0	21.6	34.8	53.3
Latent heat of vaporization KJ.kg ^{−1}	250	430	410	270

Table 4. Comparison of physicochemical properties of the three blended fuels used in the calculation.

Properties	n-Butanol/Diesel [15]	DME/Diesel [16]	DMC/Diesel [17]
Mass fraction of diesel fuel	70%	81.4%	87.8%
Mass fraction of oxygenated fuel	30%	18.6%	12.2%
Element C mass fraction	78.26%	78.08%	78.72%
Elemental O mass fraction	6.49%	6.49%	6.49%
C/O molarity ratio	16.07	16.04	16.17
Calorific value/MJ.kg ^{−1}	40.8	39.8	39.3

Table 5. Uncertainty analysis of the main apparatus used in the parameter measurement.

Property	Resolution	Uncertainty
Dynamometer (speed measurement)	1 rpm	±0.3%
Dynamometer (torque measurement)	0.01 N m	±0.2%
Flow meter sensor	0.01 g	±0.3%
Pressure transducer	0.01 MPa	±0.3%
Gas analyzer		
CO measurement	0.01%	<0.2%
HC measurement	2 ppm	<0.2%
NOx measurement	1 ppm	<0.2%

Verification of Numerical Simulation Model

In this paper, we selected Wang’s simplified n-heptane mechanism [18]. For the chemical reaction mechanism of n-butanol, the simplified kinetic mechanism for n-butanol proposed by Wang et al. [18] containing 16 components and 77 steps of reaction was selected; for the reaction mechanism of DMC, a kinetic mechanism for the chemical reaction of DMC based on a hedge diffusion flame proposed by Glaude et al. in 2005 [19], containing 102 components and 442 steps of reaction, was selected; and for DME, the chemical reaction mechanism was chosen from the detailed DME mechanism recently proposed by the Lawrence Livermore National Laboratory [20], which contains 79 components and 399 reaction steps. The stagnation periods predicted by the reaction mechanisms for these three oxygenated fuels were in good agreement with the experimental results as well as the data predicted by the detailed mechanism.

Since the carbon smoke model chosen in this study was a detailed carbon smoke model, the carbon smoke simulation needed to be based on an accurate prediction of carbon smoke precursors, so the fuel mechanism needed to contain the primordial reactions that can describe the formation of carbon smoke precursors, which directly affect the generation of the final carbon smoke, and the current domestic and international research on the chemical kinetics of PAH has also achieved certain results. We selected the model by Slavinskaya et al. [21], in which a detailed mechanism of PAH containing 93 components and 927 primordial reactions was constructed.

The three-dimensional numerical simulation platform established in this paper judged the rationality of the simulation model and the computer theory by comparing the test cylinder pressure with the simulated cylinder pressure. Figure 3 shows the comparison

between the test cylinder pressure and the simulated cylinder pressure for pure diesel fuel burning at 1800 r/min and at a 50% load. The injection pressure was 140 MPa, the injection timing was $-8.5^{\circ}\text{CA ATDC}$, and the blended fuels had an oxygen concentration of 6.49% for the n-butanol, DMC, and DME blends; according to the figure, it can be seen that the trend matched well, which indicates that the established numerical model can be used for further research calculations.

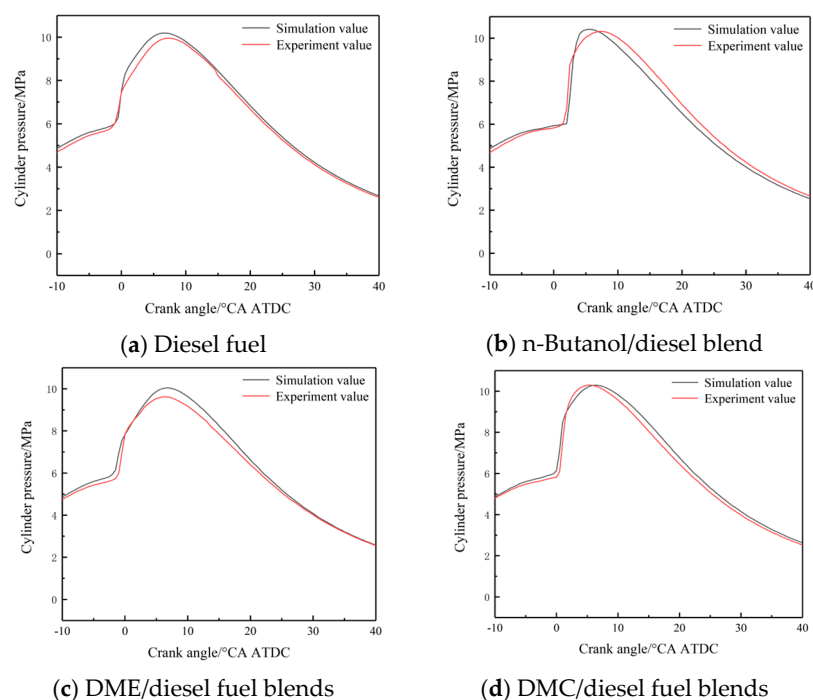


Figure 3. Comparison of test cylinder pressure and calculated cylinder pressure for each calculated fuel.

3. Results and Discussion

3.1. Effect of Different Oxygen-Containing Functional Group Fuels on Combustion

Figure 4 shows that the curves of the cylinder gas pressure (CGP) and heat release rate (HRR) for the pure diesel blended with different oxygenated fuels under medium load. It can be seen that the effect of the diesel fuel with different oxygenated fuels on the CGP and HRR of the engine under the same load was different in terms of law and degree. The DME had a higher CN than diesel fuel and a shorter ignition delay time (ID), so the CGP curve of the diesel/DME blended fuel and the pure compression curve were separated at the earliest moment, the peak HRR was the lowest, and the pressure rise was also the lowest, and the maximum burst pressure in the cylinder under medium load was 1.5% lower than that of pure diesel [22]. The CN of the DMC was lower than that of diesel, so the combustion point of the DMC/diesel blend lagged slightly behind that of diesel, and the peak HRR was higher than that of pure diesel, but in this study, the proportion of DMC blended in the diesel/DMC blend was less in order to ensure the same oxygen content, so the CN was not lower than that of pure diesel. Under medium-load conditions, the cylinder pressure curve of the n-butanol/diesel fuel blends before ignition basically coincided with that of pure diesel fuel. As compared to the three fuels, the onset time of n-butanol's combustion stage was delayed. Thus, the cylinder pressure curve exhibited an opening pattern, with a gradual increase in the peak exothermic rate, aligning with the findings of Chen Z [23]. The reason for this trend was due to the low carbon–nitrogen content of n-butanol compounds, which enhanced the blending ratio. As a result, the starting point of the combustion was delayed, resulting in a more decomposing CD mixture, the highest HRR, an appreciable increase in the in-cylinder lift, and a 2.21% increase in the maximum burst pressure with the medium load compared to diesel fuel [24].

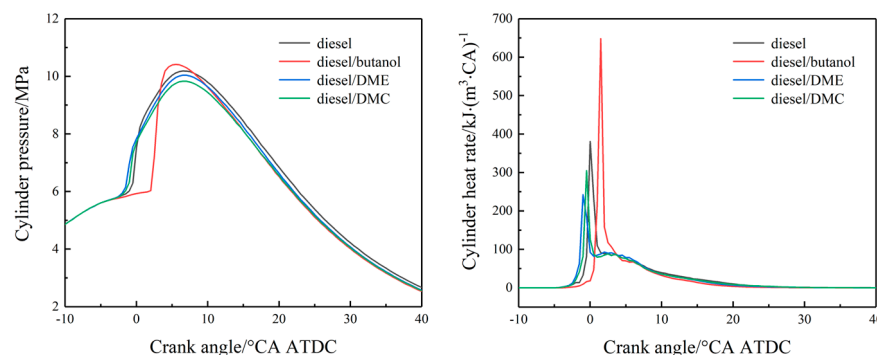


Figure 4. Comparison of CGP and HRR for different fuel blends.

3.2. ID and CD

Figure 5 shows a comparison of the combustion characteristics parameters when burning the four fuels. Again, it can be seen that the ID of the n-butanol/diesel blends was the longest. These conclusions were consistent with the findings of Wei [25]. After blending n-butanol in the diesel engine, the lagging period was prolonged, the premixed combustion quantity was increased, and the CD was shortened. This was followed by the DMC/diesel blends and pure diesel, and the ID of the DME/diesel blends was the shortest with the opposite combustion duration (CD) rule. This was because n-butanol has a lower cetane number than diesel fuel, resulting in a lower fuel ignitability and a longer ID after the addition of n-butanol, increasing the mixing time between fuel and air on the time scale, and the volatility of n-butanol is also good, so the mixture mixed more homogeneously. In addition, the amount of pre-mixed combustible mixture was increased, and the combustion rate was accelerated after the ignition, shortening the CD. The length of the ID and CD of the diesel blended with different oxygenated fuels was judged to depend mainly on the physicochemical properties of the blended fuels, as shown in Table 4.

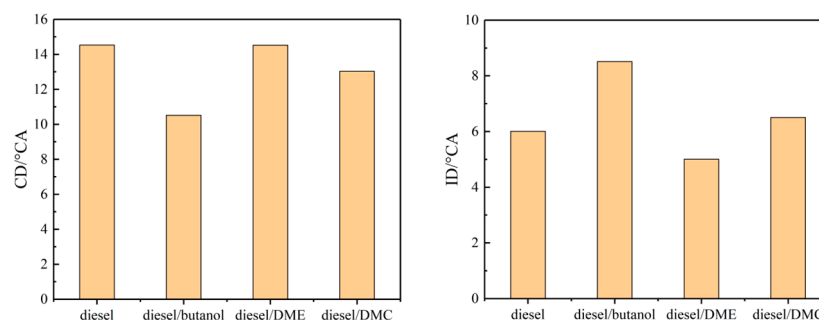


Figure 5. Comparison of combustion characteristics parameters of different fuel blends.

3.3. Effect of Different Fuels on the Main Combustion Components

In order to further understand the differences in the combustion process of the blended fuels blended with different oxygenated functional groups and also to analyze the reasons for the differences from a chemical kinetic point of view, the changes in the mass of the diesel fuel components after the addition of the different oxygenated fuels are given in Figure 6. It was found that: (1) The consumption moment and the consumption rate of n-heptane varied due to the addition of the different oxygenated fuels, with the DME/diesel blended fuel being the earliest and fastest consumed, followed by the pure diesel and DMC/diesel blends, while the n-butanol/diesel blends had the latest and slowest consumption moment of n-heptane. Therefore, it was shown that the different low-temperature activities of the oxygenated fuels influenced the low-temperature reaction of n-heptane in the blends, where the incorporation of DME improved the diesel fuel ignition at a low temperature, and the incorporation of DMC and n-butanol inhibited the diesel fuel ignition at a low temperature, and the inhibiting effect of n-butanol was more obvious [25]. (2) Comparing the generation

and consumption history of C_7H_{16} in the late stage of combustion of the different fuel blends, the consumption rate of n-heptane in the diesel/DME blends was relatively flat, indicating a higher proportion of diffusion combustion. In the reaction process of the blended fuels, n-heptane underwent dehydrogenation first, followed by n-butanol, which shows that the low-temperature activity of n-heptane is stronger than that of n-butanol, and the dehydrogenation reaction of n-heptane was gradually delayed and slowed down with the increase in the proportion of n-butanol blending. n-Heptane generated a large number of OH radicals in the low-temperature reaction stage, and some of them were occupied and consumed by n-butanol; at this time, the n-heptane and n-butanol were in competition for OH, so the low-temperature ignition of n-heptane was inhibited. This competitive relationship resulted in delayed ignition and a prolonged lag time of the fuel blend after the addition of n-butanol. Related studies have shown that the rate of chemical reaction is the main factor affecting the ignition. Zhu J [26] examined the temperature sensitivity at the instant of ignition of two fuels, n-heptane and n-heptane blended with n-butanol, utilizing the CHEMKIN 19.2 chemical analysis software, and they discovered that the essential reaction to prompt ignition remained unaffected after the admixture of the oxygenated fuels, whilst the vital reaction to suppress ignition was the dehydrogenation of n-butanol with OH radicals, reinforcing the fact that the pivotal reaction to suppress ignition was the dehydrogenation of n-butanol and OH radicals.

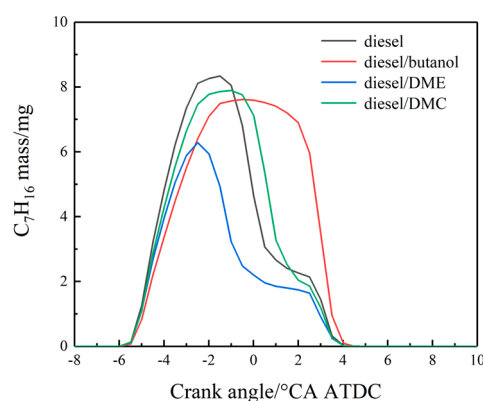


Figure 6. Change in quality diesel fuel components blended with different oxygenated fuels.

Generating a significant impact on the engine's power output, radicals, especially OH the in cylinders, promoted fuel cracking and energy release, dictating the speed and efficiency of the entire reaction sequence. Figure 7 provides a visual representation of the alteration in the radical OH mass with the different oxygenated fuels at moderate loads. This led to the following: (1) The timing of OH radical production varied for the various fuel blends. Conclusively, this highlights the superior chemical reactivity of the DME/diesel blends and the reduced reactivity of the DMC/diesel blends and n-butanol/diesel blends prior to ignition [27]. (2) Under the same fuel oxygen mass fraction, the addition of the oxygenated fuels with different structures led to different in-cylinder OH radical contents. n-Butanol produced a large amount of OH radicals due to the decomposition of H_2O_2 in the high-temperature reaction stage, resulting in the highest peak OH radical mass and the most advanced moment of reaching the peak for the n-butanol/diesel blends, the peak accumulated in-cylinder OH mass for the DMC/diesel blends being the lowest, and the peak OH accumulation for the DME/diesel blends being slightly higher than that of diesel, the reasons for which were analyzed by combining the reaction paths [28].

Figure 8 shows the main combustion oxidation pathway of DMC. It can be seen that most of the DMC and OH/O_2 underwent a dehydrogenation reaction to produce $CH_3OC(=O)OCH_2$, which is the initial reaction of the DMC oxidation process and the main reaction under high-temperature conditions; another small portion of the DMC underwent its own decomposition reaction to produce $CH_3OC(=O)O$ and CH_3 radicals.

Therefore, when burning DMC/diesel blends, the OH group content was the lowest and the in-cylinder oxidation activity was the lowest. It is worth noting that the * in the figure indicates that the substance contains double bonds.

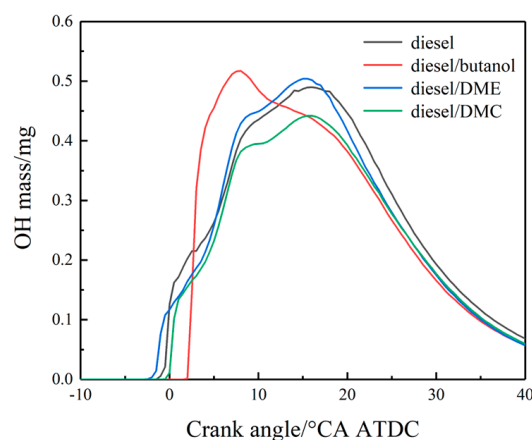


Figure 7. Variation in OH base mass for different oxygenated fuels.

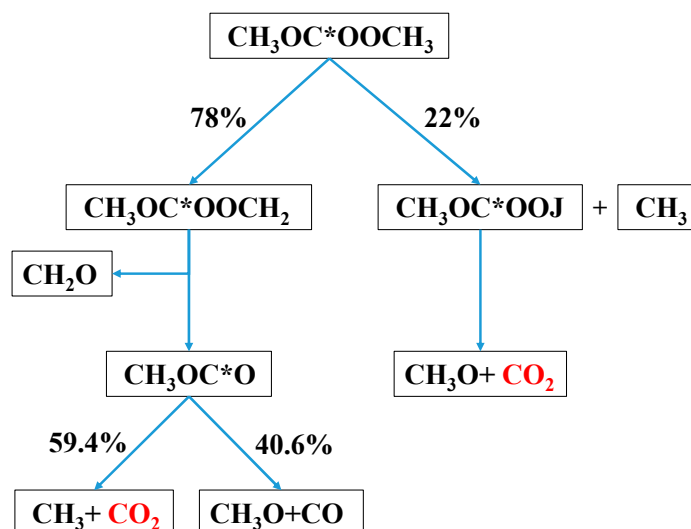


Figure 8. DMC main reaction path diagram.

Figure 9 shows the main reaction pathways for DME. The black solid line denotes the low-temperature path, while the blue solid line signifies the higher-temperature path. From the figure, it can be seen that the DME produced OH radicals important for the whole oxidation process and a large amount of formaldehyde (CH_2O) and formic acid (HCO_2) during the low-temperature reaction, and OH further promoted the low-temperature reaction, so the low-temperature activity of DME was high. A large amount of H_2O_2 also accumulated in the low-temperature reaction zone and negative-temperature-coefficient zone, and at the beginning of the high-temperature reaction, the decomposition of H_2O_2 occurred, generating OH radicals; so, as shown in Figure 8, the OH content of the DME/diesel blend fuel increased rapidly at the beginning of the high-temperature reaction, which accelerated the reaction rate of the whole system.

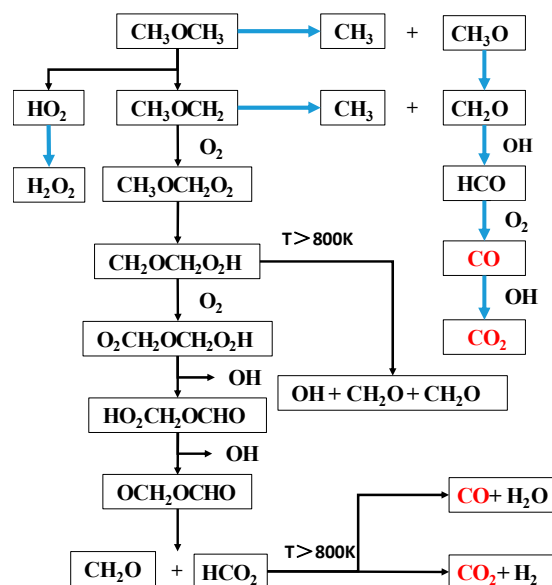


Figure 9. The main reaction path of DME.

3.4. Effect of Different Fuels on Carbon Soot Precursors

C_2H_2 and PAH, the primary precursors of carbon soot, are key to its formation. A_1 , which originally forms as an aromatic benzene ring, sets the pace for PAH. A_4 is a direct influencer of soot nucleation; hence, C_2H_2 , A_1 , and A_4 constituted the main focus of the precursors analysis in this study, as shown in Figure 10. The addition of the oxygenated fuels reduced the proportion of diesel in the fuel and also reduced the C atom content in the fuel, such that whichever oxygenated fuels were added, they could effectively reduce the formation of C_2H_2 and PAH. It can also be seen that the mass fractions of C elements in the different blends were approximately the same, indicating that the three blends were consistent in their potential to form carbon soot precursors, but it was found from the figure that due to the different structures of the oxygenated fuels, the magnitude of the reduction in C_2H_2 and PAH varied. At the same fuel oxygen content, n-butanol had the greatest ability to inhibit the formation of carbon soot precursors, which was followed by DME, and DMC had the least ability to inhibit the formation of carbon soot precursors. The reaction pathway diagrams of DME and DMC show that the DME and DMC themselves generated C_2H_4 and C_2H_2 mainly through the CH_3-CH_3 complex reaction between the methyl radicals generated in the high-temperature reaction stage, which is a shorter pathway than that of C_2H_2 generation during the oxidation of n-butanol. In addition, the O atom in the molecular structure of DME is similar to that in n-butanol, which also always combined with C atoms to generate CO, indicating that the n-butanol and DME were identical in terms of the utilization efficiency of oxygen atoms, while DMC contains three O atoms in its molecular structure, so during the reaction, most of the C=O double bonds of the DMC molecules plus another O atom directly formed CO_2 , i.e., two O atoms combined with one C atom, which reduced the utilization efficiency of O atoms, resulting in the amount of C atoms used to generate carbon soot precursors being higher in the DMC/diesel blended fuels. In addition, the oxidation of carbon soot precursors due to adding different oxygenated fuels differed, with the n-butanol/diesel blends having the highest oxidation activity, which was followed by the DME/diesel blends, and the DMC/diesel blends had the lowest. Therefore, the combination of the above aspects resulted in the highest C_2H_2 and PAH generation for the DMC/diesel blends and the lowest C_2H_2 and PAH generation for the n-butanol/diesel blends.

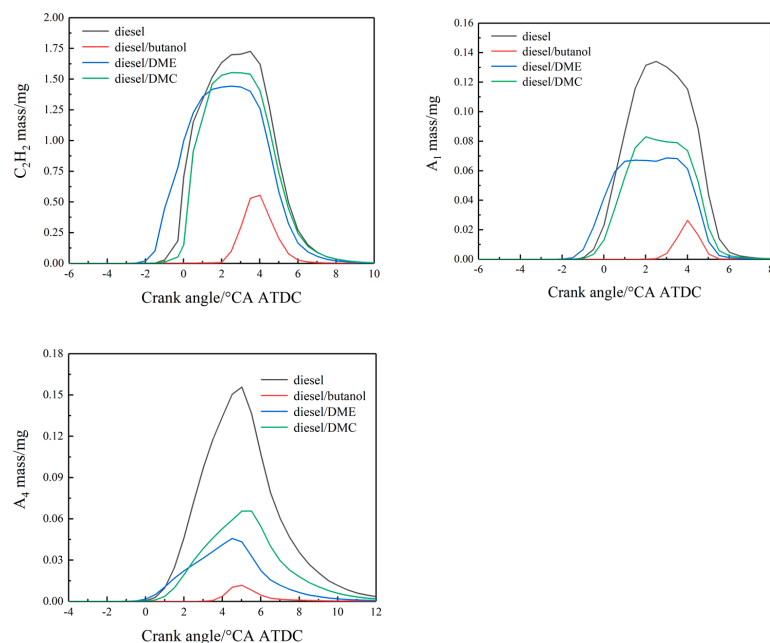


Figure 10. Changes in mass of C_2H_2 , A_1 , and A_4 for diesel blended with different fuels.

3.5. Effect of Different Fuels on the History of Soot Generation

Figure 11 illustrates the varying correlation of the soot mass to the crankshaft angle with the different fuel blends. The ultimate emission of soot represents the interplay between generation and oxidation, with elevated temperatures and oxygen deficiency being crucial influences on soot production. It is evident that the carbon soot mass exhibited an initial rise followed by a decline with the incremental change in the crankshaft angle. This was due to the fact that in the premixed phase, the generation rate of carbon smoke surpassed the oxidation rate, augmenting the carbon smoke mass until the crankshaft rotation angle reached approximately 5–10 °CA ATDC, at which point all the fuels achieved the peak value of carbon smoke. Then, with the combustion and oxidation process, the amount of oxidizing radicals in the cylinder increased, the carbon smoke generation rate was less than the oxidation rate, part of the carbon smoke was oxidized, and the carbon smoke mass decreased. From the figure, it can be seen that under the same load, the starting point of carbon soot generation was also different due to the different ignition points of blending the different oxygenated fuels, and at the same time, the peak of production of carbon soot for the different oxygenated fuel/diesel blends was also reduced to different degrees compared with pure diesel fuel. The soot peak of the diesel/DME blends was the lowest, which was followed by the diesel/DME blends, and the soot peak of diesel/DMC blends was higher than the first two blends, so the final soot emission results were as follows: pure diesel > diesel/DMC blends > diesel/DME blends > diesel/n-butanol blends. The soot emissions of the DMC, DME, and n-butanol were 8.7%, 32.6%, and 85.4% lower, respectively, than those of the pure diesel fuel under the same oxygen content. On the other hand, the OH radical content of the different oxygenated fuels was also different, which led to a difference in the in-cylinder oxidation activity, with the n-butanol/diesel combustion having the strongest oxidation activity and the DMC/diesel combustion having the weakest oxidation activity; thus, the combined effect led to the above soot emission results.

Figure 12 shows the variation in the soot mass with crankshaft angle for the different fuel blends. From the figure, it can be seen that under the same load, the starting point of carbon soot generation was also different due to the different ignition points of blending the different oxygenated fuels, and at the same time, the peak of carbon soot production for the different oxygenated fuel/diesel blends was also reduced to different degrees compared with pure diesel fuel. The soot peak of the diesel/DME blends was the lowest, which was followed by the diesel/DME blends, and the soot peak of the diesel/DMC

blends was higher than the first two blends; so, the final soot emission results were as follows: pure diesel > diesel/DMC blends > diesel/DME blends > diesel/n-butanol blends. The soot emissions of the DMC, DME, and n-butanol were 8.7%, 32.6%, and 85.4% lower, respectively, than those of pure diesel fuel under the same oxygen content. On the other hand, the OH radical content of the different oxygenated fuels was also different, which led to the difference in the in-cylinder oxidation activity, with the n-butanol/diesel combustion having the strongest oxidation activity and the DMC/diesel combustion having the weakest oxidation activity; thus, the combined effect led to the above Soot emission results [29]. After blending n-butanol fuel into diesel, the ID and volatility of the oxygenated fuel resulted in a decrease in the local mixture concentration zone. As a result, the quality of the carbon smoke generated within the cylinder was substantially reduced, producing minimal carbon smoke on the chamber walls below the throat. Moreover, at 30 °CA ATDC, the carbon smoke distributions within the cylinder were virtually nonexistent. The majority of experiments employ instrumentation to measure soot emissions, yet Ruíz F. A. [30] and Wang H. W. [31] only examined soot emission changes due to varied oxygenated fuels, overlooking soot distribution patterns within the cylinder. However, this paper compares the effect of different oxygenated functional groups on the distribution of soot in the cylinder, providing important guidance for future research.

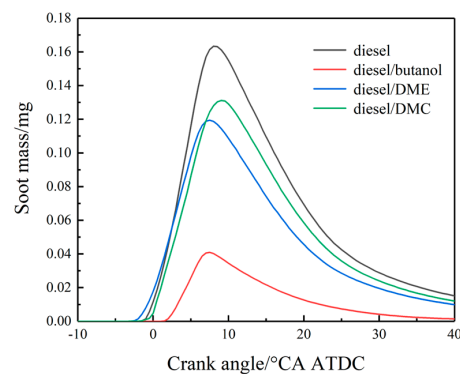


Figure 11. Changes in mass of soot for diesel blended with different fuels.

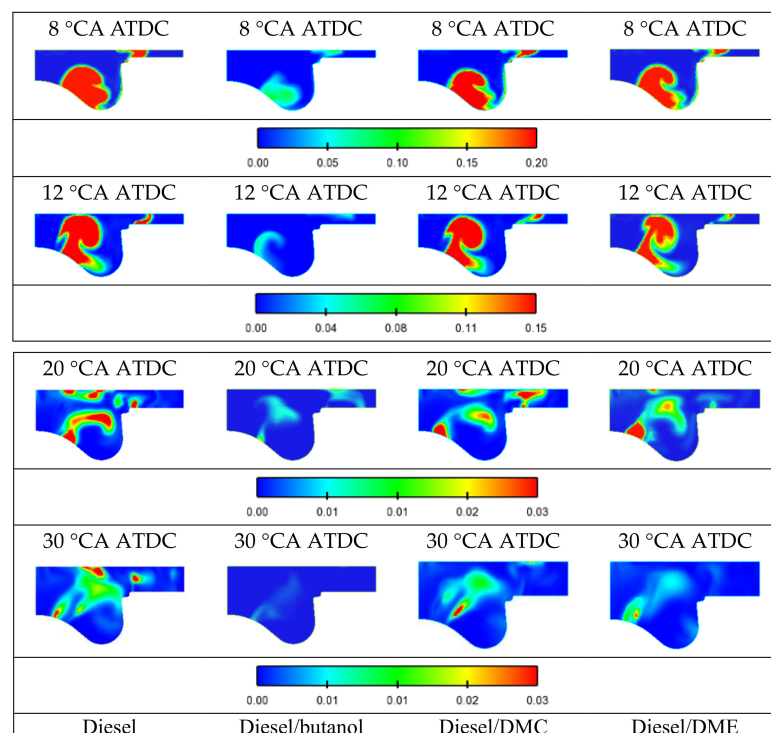


Figure 12. Soot distribution of diesel blended with fuels containing different oxygen functional groups.

3.6. Effect of Different Oxygen-Containing Functional Group Fuels on NOx Generation

Figure 13 shows the variation in the in-cylinder NOx mass with the addition of the different oxygenated fuels. It can be seen that the effect of adding the different oxygenated fuels on the NOx emissions was different. At the same load, the moment of NOx generation was delayed by the addition of the oxygenated fuels due to the prolongation of the stagnation period caused by the addition of a certain percentage of n-butanol and the relative lag at the moment when the combustion temperature reached the NOx generation temperature. As the combustion proceeded, the NOx mass did not change substantially after 20 °CA ATDC for the final NOx emissions. The air–fuel ratios of the four blends during combustion were DMC/diesel, DME/diesel, n-butanol/diesel, and pure diesel in descending order, but the in-cylinder combustion temperatures were reduced by the addition of the oxygenated fuels, and the DMC/diesel blends generated the fewest OH groups, while the n-butanol/diesel blends generated the most OH groups. According to the analysis in the previous section, the content of OH groups also affected NOx generation, so under a medium load, the NOx emissions of the n-butanol/diesel blends and DME/diesel blends were not much different from those of diesel, but the NOx emissions of the DMC/diesel blends were relatively lower, by 3.3%, compared to diesel due to the combined effect of the temperature and OH groups. Thus, the NOx emissions of the different fuel blends were all reduced to different degrees compared to pure diesel, and the NOx emissions of the added n-butanol, DME, and DMC were reduced by 0.5%, 1.7%, and 3.3%, respectively. Therefore, this study showed that DMC was more effective in reducing NOx emissions among the three oxygenated fuels.

Figure 14 shows the NOx distribution of the different fuel blends. From the figure, it can be seen that NOx was first generated at the combustion chamber pit where the high-temperature region and the low-equivalent-ratio region overlap, and a small amount was also generated at the slit position, indicating that the high-temperature and oxygen-enriched environment promoted the generation of NOx. The NOx mass concentration region also increased at 12 °C ATDC, which was determined to be due to the addition of the oxygen-containing fuels, which was equivalent to the reduction in the equivalence ratio and the higher mass of OH radicals of the mixed fuels at this time, which both resulted in an increase in the amount of NOx generation. As the combustion progressed, the NOx mass distribution gradually moved towards the entire combustion chamber in the upper part of the combustion chamber, but it was mostly focused in the middle part of the chamber, which roughly overlapped with the high-temperature region. It can be seen that the NOx distribution areas of the different fuel blends were not much different from those of pure diesel at different crankshaft angles, and the NOx mass of the diesel/DME blends was significantly less at 30 °CA ATDC. The experiments of López A F [32] and Kumar B R [33] explored the effect of different oxygenated fuels on NOx emissions, and they did not focus on the distribution of NOx in the cylinder; in addition, this paper adds a comparison of the effect of the different oxygenated functional groups on the distribution of NOx in the cylinder, which is of guiding significance in enriching the content of this study and in popularizing the engineering applications of oxygenated fuels.

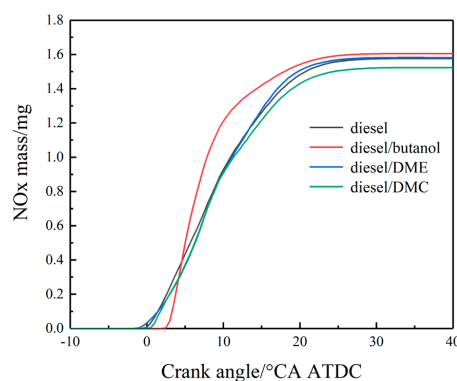


Figure 13. Comparison of nitrogen oxide emissions from diesel fuel blended with different fuels.

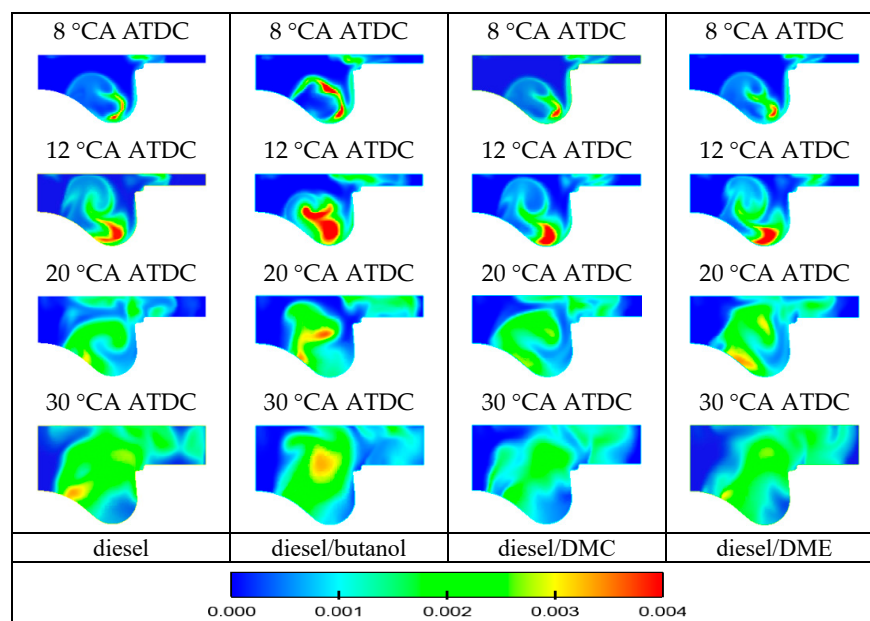


Figure 14. NO_x distribution of diesel blended with fuels containing different oxygen functional groups.

4. Conclusions

In this paper, the effects of oxygenated fuels on the combustion and emissions of a diesel engine were investigated using a built-up 3D numerical simulation platform. The combustion and emission characteristics of the oxygenated fuels with different oxygenated functional group structures added to diesel fuel with the same oxygen content of the fuel were investigated. Combined with the reaction paths of the oxygenated fuels, the development of intermediate combustion products, the main free radicals, and carbon soot precursors was analyzed in depth by using chemical reaction kinetics, and the chemical action mechanism of the different oxygenated fuels affecting the combustion and emissions was revealed. The main conclusions of this study are as follows:

(1) The influence of the oxygenated fuels on the combustion characteristics of diesel fuel was mainly manifested in the low-temperature oxidation stage. At the same fuel oxygen content, three kinds of oxygenated fuels, namely n-butanol, DME, and DMC, were added to diesel fuel, respectively, and it was found that the different low-temperature activities of the oxygenated fuels affected the low-temperature ignitability of the blended fuels in the combustion, in which DME promoted the ignition of the fuel and DMC and n-butanol suppressed the ignition. So, the length of the stagnation period was as follows: diesel/n-butanol > diesel/DMC > diesel > diesel/DME.

(2) At the same fuel oxygen content, differences in the fuel physicochemical properties and reaction paths led to different effects of the different oxygenated fuels on the in-cylinder oxidative activity and the inhibition of carbon smoke precursors. Compared with pure diesel, n-butanol and DME promoted OH generation, while DMC inhibited OH generation, so the oxidation activity of the diesel/n-butanol blend was the highest and that of the diesel/DMC blend was the lowest; meanwhile, due to the fact that the two O atoms in the DMC molecule formed CO₂ with one C atom, which reduces the efficiency of the utilization of the O atoms, its utilization efficiency of O atoms was higher, whereas each O atom in the n-butanol and DME fuels took away one C atom. The contribution ability of each oxygenated fuel to the production of carbon smoke precursors was also different, and the above combined factors led to the following ability of the oxygenated fuels to inhibit the production carbon smoke precursors under the same oxygen content: n-butanol > DME > DMC. The final soot emission results were affected by the content of carbon smoke precursors and the oxidative activity of the cylinder, and the results were as follows: pure diesel fuel > diesel/DMC blends fuel > diesel/DME blend > diesel/n-butanol blend.

(3) At medium load, the addition of n-butanol, DME, and DMC reduced NO_x emissions by 0.5%, 1.7%, and 3.3%, respectively. Thus, this study shows that DMC has a more significant effect on reducing NO_x emissions.

In order to solve the energy crisis and environmental pollution problems, countries around the world have developed increasingly stringent emissions regulations. Conventional diesel engines have limited potential to achieve ultra-low emissions due to the short mixing time of oil and gas and uneven mixing, so exploring efficient and clean combustion technology is one of the important tasks for internal combustion engine workers, and achieving efficient and clean combustion by optimizing fuel properties has been a research hotspot at home and abroad. Oxygenated fuels, as a representative of new alternative fuels, have been emphasized by researchers due to their wide range of sources and self-carrying oxygen properties. Therefore, this study was aimed at the goal of efficient and clean combustion in internal combustion engines and adopted simulation methods to change the physicochemical properties and molecular configuration of fuels by adding oxygenated fuels, such as alcohols, esters, and ethers, in order to improve the combustion and reduce emissions and to realize technological measures of efficient and clean combustion in internal combustion engines.

Author Contributions: X.L. and Y.M.: methodology, software, writing—original manuscript. Q.L. and G.W.: conceptualization, writing—review and editing. Z.Y. and Q.F.: visualization. All authors have read and agreed to the published version of the manuscript.

Funding: This work was supported by the Jilin Provincial Education Department Project (JJKH20220178KJ) and Doctoral project of Jilin Engineering Normal University (BSGC202119).

Institutional Review Board Statement: Not applicable.

Informed Consent Statement: Not applicable.

Data Availability Statement: The data that support the findings of this study are available from the corresponding author upon reasonable request.

Acknowledgments: We are very grateful to the Jilin Provincial Government and Jilin Engineering Teachers College for funding this thesis.

Conflicts of Interest: The authors declare no conflict of interest. There are no known financial interests or personal relationships that may have influenced the work reported herein.

References

1. Wu, H.; Xie, F.; Han, Y.; Zhang, Q.; Li, Y. Effect of cetane coupled injection parameters on diesel engine combustion and emissions. *Fuel* **2022**, *319*, 123714. [\[CrossRef\]](#)
2. Vargün, M.; Özsezen, A.N. Evaluation of the effect of the fuel injection phase on the combustion and exhaust characteristics in a diesel engine operating with alcohol-diesel mixtures. *Energy* **2023**, *270*, 126975. [\[CrossRef\]](#)
3. Yesilyurt, M.K.; Aydin, M.; Yilbasi, Z.; Arslan, M. Investigation on the structural effects of the addition of alcohols having various chain lengths into the vegetable oil-biodiesel-diesel fuel blends: An attempt for improving the performance, combustion, and exhaust emission characteristics of a compression ignition engine. *Fuel* **2020**, *269*, 117455. [\[CrossRef\]](#)
4. Yesilyurt, M.K.; Yilbasi, Z.; Aydin, M. The performance, emissions, and combustion characteristics of an unmodified diesel engine running on the ternary blends of pentanol/safflower oil biodiesel/diesel fuel. *J. Therm. Anal. Calorim.* **2020**, *140*, 2903–2942. [\[CrossRef\]](#)
5. Sun, P.; Feng, J.; Yang, S.; Wang, C.; Cui, K.; Dong, W.; Du, Y.; Yu, X.; Zhou, J. Particulate number and size distribution of dimethyl ether/gasoline combined injection spark ignition engines at medium engine speed and load. *Fuel* **2022**, *315*, 122645. [\[CrossRef\]](#)
6. Putrasari, Y.; Lim, O. Dimethyl ether as the next generation fuel to control nitrogen oxides and particulate matter emissions from internal combustion engines: A review. *ACS Omega* **2021**, *7*, 32–37. [\[CrossRef\]](#)
7. Yilbaşı, Z.; Yeşilyurt, M.K.; Arslan, M.; Yaman, H. Understanding the performance, emissions, and combustion behaviors of a DI diesel engine using alcohol/hemp seed oil biodiesel/diesel fuel ternary blends: Influence of long-chain alcohol type and concentration. *Sci. Technol. Energy Transit.* **2023**, *78*, 5. [\[CrossRef\]](#)
8. Huang, W.; Pratama, R.H.; Oguma, M.; Kinoshita, K.; Takeda, Y.; Suzuki, S. Spray dynamics of synthetic dimethyl carbonate and its blends with gasoline. *Fuel* **2023**, *341*, 127696. [\[CrossRef\]](#)
9. Kim, H.J.; Park, S.H. Optimization study on exhaust emissions and fuel consumption in a dimethyl ether (DME) fueled diesel engine. *Fuel* **2016**, *182*, 541–549. [\[CrossRef\]](#)

10. Wu, H.; Xie, F.; Han, Y. Effect of cetane coupled with various engine conditions on diesel engine combustion and emission. *Fuel* **2022**, *322*, 124164. [\[CrossRef\]](#)
11. Wang, H.; Ji, C.; Shi, C.; Ge, Y.; Meng, H.; Yang, J.; Chang, K.; Wang, S. Comparison and evaluation of advanced machine learning methods for performance and emissions prediction of a gasoline Wankel rotary engine. *Energy* **2022**, *248*, 123611. [\[CrossRef\]](#)
12. Li, M.; Xu, Z.; Luo, Q.; Wang, C. Investigation of bicubic flame radiation model of continuously opposed spilling fire over n-butanol fuel. *Energy* **2023**, *272*, 127144. [\[CrossRef\]](#)
13. Agarwal, A.K.; Kumar, V.; Valera, H.; Mukherjee, N.K.; Mehra, S.; Nene, D. Ultra-low soot/particulate emissions from a dimethyl ether-fueled agricultural tractor engine. *Fuel* **2024**, *356*, 129637. [\[CrossRef\]](#)
14. Sun, W.; Zhu, G.; Guo, L.; Zhang, H.; Yan, Y.; Lin, S.; Zeng, W.; Zhang, X.; Jiang, M.; Yu, C. Optical diagnostic study of internal and external EGR combined with oxygenated fuels of n-butanol, PODE3 and DMC to optimize the combustion process of FT synthetic diesel. *Fuel* **2024**, *355*, 129390. [\[CrossRef\]](#)
15. Gao, S.; Zhang, Y.; Zhang, Z.; Tan, D.; Li, J.; Yin, Z.; Hu, J.; Zhao, Z. Multi-objective optimization of the combustion chamber geometry for a highland diesel engine fueled with diesel/n-butanol/PODEn by ANN-NSGA III. *Energy* **2023**, *282*, 128793. [\[CrossRef\]](#)
16. Tripathi, A.; Agarwal, A.K. Characterisation of particulates and trace metals emitted by a dimethyl ether-fuelled genset engine prototype. *Environ. Pollut.* **2023**, *329*, 121649. [\[CrossRef\]](#)
17. Li, M.D.; Wang, Z.; Liu, S.A.; Li, R.N.; Zhao, Y. Study on the Particulate Microstructure of Different Oxygenated Fuels. *Adv. Mater. Res.* **2013**, *726*, 1950–1953. [\[CrossRef\]](#)
18. Wang, H.; Deneyts Reitz, R.; Yao, M.; Yang, B.; Jiao, Q.; Qiu, L. Development of an n-heptane-n-butanol-PAH mechanism and its application for combustion and soot prediction. *Combust. Flame* **2013**, *160*, 504–519. [\[CrossRef\]](#)
19. Glaude, P.A.; Pitz, W.J.; Thomson, M.J. Chemical kinetic modeling of dimethyl carbonate in an opposed-flow diffusion flame. *Proc. Combust. Inst.* **2005**, *30*, 1111–1118. [\[CrossRef\]](#)
20. Kaiser, E.W.; Wallington, T.J.; Hurley, M.D.; Platz, J.; Curran, H.J.; Pitz, W.J.; Westbrook, C.K. Experimental and Modeling Study of Premixed Atmospheric-Pressure Dimethyl Ether–Air Flames. *J. Phys. Chem. A* **2000**, *104*, 8194–8206. [\[CrossRef\]](#)
21. Slavinskaya, N.; Frank, P. A modelling study of aromatic soot precursors formation in laminar methane and ethene flames. *Combust. Flame* **2009**, *156*, 1705–1722. [\[CrossRef\]](#)
22. Labeckas, G.; Slavinskis, S.; Rudnicki, J.; Zadrag, R. The effect of oxygenated diesel-n-butanol fuel blends on combustion, performance, and exhaust emissions of a turbocharged CRDI diesel engine. *Pol. Marit. Res.* **2018**, *25*, 108–120. [\[CrossRef\]](#)
23. Choi, B.; Jiang, X.; Kim, Y.K.; Jung, G.; Lee, C.; Choi, I.; Song, C.S. Effect of diesel fuel blend with n-butanol on the emission of a turbocharged common rail direct injection diesel engine. *Appl. Energy* **2015**, *146*, 20–28. [\[CrossRef\]](#)
24. Chen, Z.; Wu, Z.; Liu, J.; Lee, C. Combustion and emissions characteristics of high n-butanol/diesel ratio blend in a heavy-duty diesel engine and EGR impact. *Energy Convers. Manag.* **2014**, *78*, 787–795. [\[CrossRef\]](#)
25. Wei, L.; Cheung, C.; Huang, Z. Effect of n-pentanol addition on the combustion, performance and emission characteristics of a direct-injection diesel engine. *Energy* **2014**, *70*, 172–180. [\[CrossRef\]](#)
26. Zhu, J.; Huang, H.; Zhu, Z.; Lv, D.; Pan, Y.; Wei, H.; Zhuang, J. Effect of intake oxygen concentration on diesel–n-butanol blending combustion: An experimental and numerical study at low engine load. *Energy Convers. Manag.* **2018**, *165*, 53–65. [\[CrossRef\]](#)
27. Rahiman, M.K.; Santhoshkumar, S.; Subramaniam, D.; Avinash, A.; Pugazhendhi, A. Effects of oxygenated fuel pertaining to fuel analysis on diesel engine combustion and emission characteristics. *Energy* **2022**, *239*, 122373. [\[CrossRef\]](#)
28. Alptekin, E. Emission, injection and combustion characteristics of biodiesel and oxygenated fuel blends in a common rail diesel engine. *Energy* **2017**, *119*, 44–52. [\[CrossRef\]](#)
29. Abdalla, A.O.G.; Liu, D. Dimethyl carbonate as a promising oxygenated fuel for combustion: A review. *Energies* **2018**, *11*, 1552. [\[CrossRef\]](#)
30. Ruiz, F.A.; Cadrazco, M.; López, A.F.; Sanchez-Valdepeñas, J.; Agudelo, J.R. Impact of dual-fuel combustion with n-butanol or hydrous ethanol on the oxidation reactivity and nanostructure of diesel particulate matter. *Fuel* **2015**, *161*, 18–25. [\[CrossRef\]](#)
31. Wang, H.W.; Huang, Z.H.; Zhou, L.B.; Jiang, D.M.; Yang, Z.L. Technical note: Investigation on emission characteristics of a compression ignition engine with oxygenated fuels and exhaust gas recirculation. *Proc. Inst. Mech. Eng. Part D J. Automob. Eng.* **2005**, *214*, 503–508. [\[CrossRef\]](#)
32. López, A.F.; Cadrazco, M.; Agudelo, A.F.; Corredor, L.A.; Vélez, J.A.; Agudelo, J.R. Impact of n-butanol and hydrous ethanol fumigation on the performance and pollutant emissions of an automotive diesel engine. *Fuel* **2015**, *153*, 483–491. [\[CrossRef\]](#)
33. Kumar, B.R.; Saravanan, S. Partially premixed low temperature combustion using dimethyl carbonate (DMC) in a DI diesel engine for favorable smoke/NOx emissions. *Fuel* **2016**, *180*, 396–406. [\[CrossRef\]](#)

Disclaimer/Publisher’s Note: The statements, opinions and data contained in all publications are solely those of the individual author(s) and contributor(s) and not of MDPI and/or the editor(s). MDPI and/or the editor(s) disclaim responsibility for any injury to people or property resulting from any ideas, methods, instructions or products referred to in the content.